Arthur E. Rowland
University of Detroit.

NATIONAL ADVISORY COMMITTEE FOR AERONAUTICS

REPORT No. 527

AIR FLOW IN A SEPARATING LAMINAR BOUNDARY LAYER

By G. B. SCHUBAUER

The Garrett Corporation
AiResearch Mfg. Div.
SEP 2 1975
LIBRARY

1935

For sale by the Superintendent of Documents, Washington, D. C. - - - - - - - - - - - - - - Price 5 cents

AERONAUTIC SYMBOLS

1. FUNDAMENTAL AND DERIVED UNITS

	Symbol	Metric		English	
		Unit	Abbreviation	Unit	Abbreviation
Length	l	meter	m	foot (or mile)	ft. (or mi.)
Time	t	second	s	second (or hour)	sec. (or hr.)
Force	F	weight of 1 kilogram	kg	weight of 1 pound	lb.
Power	P	horsepower (metric)		horsepower	hp.
Speed	V	kilometers per hour	k.p.h.	miles per hour	m.p.h.
		meters per second	m.p.s.	feet per second	f.p.s.

2. GENERAL SYMBOLS

W, Weight $= mg$

g, Standard acceleration of gravity $= 9.80665$ m/s^2 or 32.1740 ft./sec.^{2}

m, Mass $= \frac{W}{g}$

I, Moment of inertia $= mk^2$. (Indicate axis of radius of gyration k by proper subscript.)

μ, Coefficient of viscosity

ν, Kinematic viscosity

ρ, Density (mass per unit volume)

Standard density of dry air, 0.12497 kg-m^{-4}-s^2 at 15° C. and 760 mm; or 0.002378 lb.-ft.$^{-4}$ sec.^{2}

Specific weight of "standard" air, 1.2255 kg/m^3 or 0.07651 lb./cu.ft.

3. AERODYNAMIC SYMBOLS

S, Area

S_w, Area of wing

G, Gap

b, Span

c, Chord

$\frac{b^2}{S}$, Aspect ratio

V, True air speed

q, Dynamic pressure $= \frac{1}{2}\rho V^2$

L, Lift, absolute coefficient $C_L = \frac{L}{qS}$

D, Drag, absolute coefficient $C_D = \frac{D}{qS}$

D_o, Profile drag, absolute coefficient $C_{D_o} = \frac{D_o}{qS}$

D_i, Induced drag, absolute coefficient $C_{D_i} = \frac{D_i}{qS}$

D_p, Parasite drag, absolute coefficient $C_{D_p} = \frac{D_p}{qS}$

C, Cross-wind force, absolute coefficient $C_C = \frac{C}{qS}$

R, Resultant force

i_w, Angle of setting of wings (relative to thrust line)

i_t, Angle of stabilizer setting (relative to thrust line)

Q, Resultant moment

Ω, Resultant angular velocity

$\frac{\rho V l}{\mu}$, Reynolds Number, where l is a linear dimension (e.g., for a model airfoil 3 in. chord, 100 m.p.h. normal pressure at 15° C., the corresponding number is 234,000; or for a model of 10 cm chord, 40 m.p.s. the corresponding number is 274,000)

C_p, Center-of-pressure coefficient (ratio of distance of $c.p.$ from leading edge to chord length)

α, Angle of attack

ϵ, Angle of downwash

α_o, Angle of attack, infinite aspect ratio

α_i, Angle of attack, induced

α_a, Angle of attack, absolute (measured from zero-lift position)

γ, Flight-path angle

REPORT No. 527

AIR FLOW IN A SEPARATING LAMINAR BOUNDARY LAYER

By G. B. SCHUBAUER
National Bureau of Standards

122956—35

NATIONAL ADVISORY COMMITTEE FOR AERONAUTICS

HEADQUARTERS, NAVY BUILDING, WASHINGTON, D. C.

LABORATORIES, LANGLEY FIELD, VA.

Created by act of Congress approved March 3, 1915, for the supervision and direction of the scientific study of the problems of flight. Its membership was increased to 15 by act approved March 2, 1929. The members are appointed by the President, and serve as such without compensation.

JOSEPH S. AMES, Ph. D., *Chairman*,
President, Johns Hopkins University, Baltimore, Md.

DAVID W. TAYLOR, D. Eng., *Vice Chairman*.
Washington, D. C.

CHARLES G. ABBOT, Sc. D.,
Secretary, Smithsonian Institution.

LYMAN J. BRIGGS, Ph. D.,
Director, National Bureau of Standards.

BENJAMIN D. FOULOIS, Major General, United States Army,
Chief of Air Corps, War Department.

WILLIS RAY GREGG, B. A.,
Chief, United States Weather Bureau.

HARRY F. GUGGENHEIM, M. A.,
Port Washington, Long Island, N. Y.

ERNEST J. KING, Rear Admiral, United States Navy,
Chief, Bureau of Aeronautics, Navy Department.

CHARLES A. LINDBERGH, LL. D.,
New York City.

WILLIAM P. MACCRACKEN, Jr., Ph. B.,
Washington, D. C.

AUGUSTINE W. ROBINS, Brig. Gen., United States Army,
Chief, Matériel Division, Air Corps, Wright Field, Dayton, Ohio.

EUGENE L. VIDAL, C. E.,
Director of Air Commerce, Department of Commerce.

EDWARD P. WARNER, M. S.,
Editor of Aviation, New York City.

R. D. WEYERBACHER, Commander, United States Navy,
Bureau of Aeronautics, Navy Department.

ORVILLE WRIGHT, Sc. D.,
Dayton, Ohio.

GEORGE W. LEWIS, *Director of Aeronautical Research*

JOHN F. VICTORY, *Secretary*

HENRY J. E. REID, *Engineer in Charge, Langley Memorial Aeronautical Laboratory, Langley Field, Va.*

JOHN J. IDE, *Technical Assistant in Europe, Paris, France*

TECHNICAL COMMITTEES

AERODYNAMICS
POWER PLANTS FOR AIRCRAFT
AIRCRAFT STRUCTURES AND MATERIALS
AIRCRAFT ACCIDENTS
INVENTIONS AND DESIGNS

Coordination of Research Needs of Military and Civil Aviation

Preparation of Research Programs

Allocation of Problems

Prevention of Duplication

Consideration of Inventions

LANGLEY MEMORIAL AERONAUTICAL LABORATORY

LANGLEY FIELD, VA.

Unified conduct, for all agencies, of scientific research on the fundamental problems of flight.

OFFICE OF AERONAUTICAL INTELLIGENCE

WASHINGTON, D. C.

Collection, classification, compilation, and dissemination of scientific and technical information on aeronautics.

REPORT No. 527

AIR FLOW IN A SEPARATING LAMINAR BOUNDARY LAYER

By G. B. Schubauer

SUMMARY

The speed distribution in a laminar boundary layer on the surface of an elliptic cylinder, of major and minor axes 11.78 and 3.98 inches, respectively, has been determined by means of a hot-wire anemometer. The direction of the impinging air stream was parallel to the major axis. Special attention was given to the speed distribution in the region of separation and to the exact location of the point of separation. An approximate method, developed by K. Pohlhausen for computing the speed distribution, the thickness of the layer, and the point of separation, is described in detail; and speed-distribution curves calculated by this method are presented for comparison with experiment. Good agreement is obtained along the forward part of the cylinder, but Pohlhausen's method fails shortly before the separation point is reached and consequently cannot be used to locate this point.

The work was carried out at the National Bureau of Standards with the cooperation and financial assistance of the National Advisory Committee for Aeronautics.

INTRODUCTION

Prandtl's postulate, that the viscosity of the fluid plays an important role only in a thin "boundary layer" on the surface of a body in a moving fluid, has been the key to the understanding of many puzzling phenomena occurring in the flow of viscous fluids. Subsequent works, both experimental and theoretical, have verified the existence of a "boundary layer" and have given conclusive evidence that the radical difference between the behavior of an ideal fluid and that of a viscous fluid is due to the presence of a boundary layer and the wake resulting from its separation from the surface of the body.

In the region of potential flow outside the boundary layer and wake the effect of viscosity is negligible; hence the mathematical theory pertaining to the flow of a nonviscous fluid may be applied, a procedure which obviously finds greatest application in the treatment of flow about body forms on which separation is delayed and for which the wake is small. While the flow within the boundary layer must be treated as viscous, much of the difficulty was avoided by Prandtl, who derived a general equation of motion on the assumption that the boundary layer is thin compared to the dimensions of the body. Thus, excluding the wake, it might appear possible to work with two regions, one being the boundary layer and the other the region outside, each governed by its own set of laws. A more careful consideration shows, however, that each has an effect upon the other, and that no satisfactory solution of the problem as a whole can be obtained without treating the two simultaneously. At present this is impossible.

It has been found that the velocity distribution in the boundary layer, its thickness, and its tendency to separate from the surface of the body are governed almost entirely by the velocity distribution in the region of potential flow outside the layer. The procedure adopted, therefore, is to measure the velocity distribution outside the layer and to use this as a basis for calculating the flow within the layer itself. This procedure takes the place of the familiar one used in potential theory, that of using the shape of the body as the basis. A treatment of the former type, employing the Kármán integral equation, has been developed by K. Pohlhausen (reference 1). Unfortunately this treatment is approximate and experimental data are necessary to test the validity of the assumptions made.

The flow in the boundary layer described by Prandtl's equation is termed "laminar flow." It is well known that as the layer thickens this type of flow breaks down and is replaced by turbulent flow. If it be desired to maintain laminar flow, transition to the turbulent state may always be avoided by a sufficient lowering of the Reynolds Number.

The present paper describes a study of the flow in a laminar boundary layer formed in the two-dimensional flow around an elliptic cylinder oriented with its major axis parallel to the air stream of a wind tunnel. Measurements of the speed distribution in the layer have been made by means of a hot-wire anemometer, and extend from the origin of the layer to and beyond the region where it separates from the surface of the cylinder. The Reynolds Number has been so chosen that the flow in the boundary layer does not become turbulent before separation. The purpose of the study was to test Pohlhausen's approximate solution of the Kármán integral equation, especially in the region of separation.

While a treatment of boundary-layer theory may readily be found in the literature (for example, in reference 1, which includes also Pohlhausen's solution) a brief discussion is included for conveniently judging the validity of the approximations as applied to the problem at hand.

I. DEFINITIONS OF SYMBOLS

We shall adopt a curvilinear system of coordinates in which x denotes distance along the curved surface of the elliptic cylinder measured from the forward stagnation point and y distance normal to and measured from the surface. The radius of curvature of the surface, and hence of the x axis, will be denoted by r. Since y will always be small, we shall neglect its curvature. The x and y components of velocity in the boundary layer will be denoted by u and v, respectively, and the x component of velocity just outside the boundary layer, by U. The pressure of the air at any point in the layer will be denoted by p.

We shall find it convenient at the outset to express distances, speeds, and pressure in terms of corresponding reference quantities as the units, denoted respectively, by L, U_0 and P_0. The minor axis of the ellipse (L=3.98 inches) is selected as the reference length. The speed of the undisturbed stream of the wind tunnel is chosen as the reference speed; that is, the air speed that would prevail in the empty tunnel at the position to be occupied by the leading edge (forward stagnation point) of the elliptic cylinder (U_0, about 11.5 feet per second). The reference pressure (really a pressure difference) conveniently follows as the pressure rise when air of initial speed U_0 is brought to rest by impact, i. e., $P_0=\frac{1}{2}\rho U_0^2$, where ρ is the air density. The Reynolds Number R is defined as $\frac{LU_0}{\nu}$, where ν is the kinematic viscosity of the air.

The foregoing quantities are made dimensionless as follows:

$$\frac{x}{L}, \frac{y}{L}, \frac{r}{L}, \frac{u}{U_0}, \frac{v}{U_0}, \frac{p}{P_0}=\frac{p}{\frac{1}{2}\rho U_0^2}$$

In order to avoid writing quotients, the symbols x, y, r, u, v, U, and p will be used to denote dimensionless quantities in the remainder of the paper, the division by the appropriate reference quantity being inferred. The symbols with their new meaning are summarized as follows:

- L, Length of minor axis of elliptic cylinder.
- x, Distance along the curved surface of the elliptic cylinder at right angles to the axis of the cylinder and measured from the forward stagnation point, divided by L.
- y, Distance normal to and measured from the surface divided by L.
- r, Radius of curvature of the surface divided by L.
- u, x component of velocity in the boundary layer divided by U_0.
- U, x component of velocity in the region of potential flow just outside the boundary layer divided by U_0.
- v, y component of velocity in the boundary layer divided by U_0.
- p, Pressure of the air divided by P_0.

For describing the separated boundary layer x_b and y_b are introduced.

- x_b, Distance divided by L, the same as x up to the point of separation, but parallel to the major axis of the ellipse beyond this point.
- y_b, Distance divided by L perpendicular to x_b, with origin on the major axis of the ellipse or the major axis produced.

(x_b, y_b) is any point aft of the separation point.

Figure 13 may help the reader to visualize some of the foregoing quantities.

II. BOUNDARY LAYER THEORY

1. GENERAL EQUATION

The experimental conditions, a steady two-dimensional flow of air at speeds so low that compressibility may be neglected, makes possible an immediate simplification of the Navier-Stokes equations (reference 2). Their simplified and appropriate form, given by Fuchs-Hopf (reference 3) in our particular curvilinear coordinate system and written here nondimensionally, is

$$u\frac{\partial u}{\partial x}+v\frac{\partial u}{\partial y}-\frac{uv}{r}=\frac{1}{R}\left(\frac{\partial^2 u}{\partial x^2}+\frac{\partial^2 u}{\partial y^2}-\frac{1}{r}\frac{\partial u}{\partial y}-\frac{2}{r}\frac{\partial v}{\partial x}-\frac{u}{r^2}+\frac{v}{r^2}\frac{\partial r}{\partial x}\right)-\frac{1}{2}\frac{\partial p}{\partial x} \tag{1}$$

$$u\frac{\partial v}{\partial x}+v\frac{\partial v}{\partial y}+\frac{u^2}{r}=\frac{1}{R}\left(\frac{\partial^2 v}{\partial x^2}+\frac{\partial^2 v}{\partial y^2}+\frac{2}{r}\frac{\partial u}{\partial x}+\frac{1}{r}\frac{\partial v}{\partial y}-\frac{u}{r^2}\frac{\partial r}{\partial x}-\frac{v}{r^2}\right)-\frac{1}{2}\frac{\partial p}{\partial y} \tag{2}$$

These together with the equation of continuity

$$\frac{\partial u}{\partial x}+\frac{\partial v}{\partial y}-\frac{v}{r}=0 \tag{3}$$

are the equations of motion of a viscous fluid from which a mathematical treatment of boundary-layer flow may begin.

A boundary-layer equation was derived by Prandtl (reference 4) from equations in rectangular coordinates corresponding to (1), (2), and (3) by neglecting terms that become unimportant when the treatment is applied to a thin layer of thickness δ (δ is also expressed with L as the unit). The terms that may be neglected were found by a consideration of relative orders of magnitude. Although the quantities retained are, on the average, of a higher order of magnitude than those neglected, in certain regions some of the former assume

very small values and even change sign. In these regions some of the neglected quantities may be of a higher order than some of those retained but, from the form of the equations, it does not appear that this will introduce any significant additional uncertainty. The ultimate test of the accuracy of the approximation formulas is the agreement between calculation and observation.

In the following discussion we shall use the expression "of the order of" (designated by the symbol 0) to mean the maximum order attained by a given quantity. For example, when u is said to be 0 (1), u may reach values ± 1 or even ± 10, but it may at times have much smaller numerical values, even zero. A factor of 10, or possibly greater, is not to be considered as sufficient to change the order of magnitude but a factor of, let us say, 100 places the quantity in a higher order.

Experimentally we find sufficient justification for writing

$$x,\ r^1,\ u,\ U,\ \frac{\partial u}{\partial x}\ \frac{\partial^2 u}{\partial x^2} \text{ and } \frac{\partial U}{\partial x} \text{ are } 0\ (1)$$

$$\frac{\partial u}{\partial y} \text{ is } 0\left(\frac{1}{\delta}\right)$$

$$\frac{\partial^2 u}{\partial y^2} \text{ is } 0\left(\frac{1}{\delta^2}\right)$$

From Bernoulli's theorem ($p+U^2=$constant, bearing in mind that this equation is in dimensionless form)

$$\frac{\partial p}{\partial x} \text{ is } 0\ (1)$$

Equation (3) indicates that $\frac{\partial v}{\partial y}-\frac{v}{r}$ is 0 (1). Since v can safely be assumed to be $0(\delta)$, $\frac{\partial v}{\partial y}$ must be $0(1)$. Consideration of the order of mangitude of v indicates that it is a reasonable assumption to assign values $0(\delta)$ to $\frac{\partial v}{\partial x}$ and $\frac{\partial^2 v}{\partial x^2}$, and a value $0\left(\frac{1}{\delta}\right)$ to $\frac{\partial^2 v}{\partial y^2}$.

Equations (1) and (2) are now rewritten with orders of magnitude replacing the terms themselves, except for R and $\frac{\partial p}{\partial y}$ which are as yet undetermined.

$$0(1)+0(1)-0(\delta)=\frac{1}{R}[0(1)+0\left(\frac{1}{\delta^2}\right)-0\left(\frac{1}{\delta}\right)-0(\delta)-0(1)+0(\delta)]-0(1) \tag{1a}$$

$$0(\delta)+0(\delta)+0(1)=\frac{1}{R}[0(\delta)+0\left(\frac{1}{\delta}\right)+0(1)+0(1)-0(1)-0(\delta)]-\frac{1}{2}\frac{\partial p}{\partial y} \tag{2a}$$

[1] r for the elliptic cylinder goes from 0.17 at the leading edge to 4.4 at the thickest section.

In the boundary layer the inertial and frictional forces are assumed to be of nearly equal importance; hence the inertial and frictional terms in equations (1) and (2) must be of the same order of magnitude. In order to satisfy this requirement, δ must be such that R in equation (1a) is $0\left(\frac{1}{\delta^2}\right)$; and, to satisfy equation (2a) at the same time, $\frac{\partial p}{\partial y}$ must be 0 (1).

The assumption of a thin layer means that δ is small compared to 1, and hence that terms 0 (δ) or smaller may be neglected. When this is done, equation (1) becomes

$$u\frac{\partial u}{\partial x}+v\frac{\partial u}{\partial y}=\frac{1}{R}\frac{\partial^2 u}{\partial y^2}-\frac{1}{2}\frac{\partial p}{\partial x} \tag{4}$$

and equation (2), while of no importance in the discussion to follow other than to indicate that $\frac{\partial p}{\partial y}$ is 0 (1), becomes

$$-\frac{1}{2}\frac{\partial p}{\partial y}=\frac{u^2}{r}$$

Equation (3) reduces to

$$\frac{\partial u}{\partial x}+\frac{\partial v}{\partial y}=0 \tag{5}$$

Equation (4) is the boundary-layer equation as originally derived by Prandtl.

Two additional results have come out of the preceding discussion. The first, that $\frac{1}{\delta^2}$ is 0 (R), not only indicates one experimental requirement for the validity of equation (4) but shows us, to order of magnitude at least, that δ varies as $\frac{1}{\sqrt{R}}$ when equation (4) is valid. By momentum considerations the law is actually found to be $\delta=K\frac{1}{\sqrt{R}}$, where K is an unknown constant of 0 (1). The second, that $\frac{\partial p}{\partial y}$ is 0 (1), shows that the change in pressure across the boundary layer from $y=0$ to $y=\delta$ is 0 (δ). The significance of the latter deduction is that a pressure measured at some point on the surface of the cylinder may be regarded as the pressure in the boundary layer and in the potential flow just beyond it, anywhere along the normal to the surface from that point, and hence may be used to compute the speed in the potential flow by Bernoulli's equation.

At the surface u and v are zero. As y increases, u asymptotically approaches U, the speed in potential flow outside the boundary layer. U is usually a function of x; and just beyond the boundary layer may be regarded as a function of x alone, its change with y in the potential flow being of a lower order of magnitude than within the boundary layer.

In potential flow we have by Bernoulli's theorem

$$p+U^2=p_0+U_0^2$$

where p and p_0 are the dimensionless pressure for the points with the dimensionless velocities U and U_0, respectively. We shall choose for U_0 the speed of the undisturbed stream; and when we do so, we note, upon reference to section I, that its value is unity. We observe also that p_0 is a constant. Replacing U_0 by unity and solving for U, we obtain

$$U^2=1-(p-p_0) \tag{6}$$

Equation (6) is a relation between the dimensionless pressure and the dimensionless speed at the outer boundary of the layer. Differentiating equation (6) with respect to x and denoting $\frac{dU}{dx}$ by U' yields

$$-\frac{dp}{dx}=2UU' \tag{7}$$

Neglecting a pressure difference 0 (δ), the pressure at the surface and its variation with x are related to U and U' by equations (6) and (7).

Using equations (4), (5), and (7) an integral equation, namely, the "Kármán integral equation", may be developed (reference 1). It is expressed as follows:

$$-2U'\int_0^\infty (U-u)dy-U\frac{d}{dx}\int_0^\infty (U-u)dy +\frac{d}{dx}\int_0^\infty (U-u)^2dy=-\frac{1}{R}\left(\frac{\partial u}{\partial y}\right)_{y=0} \tag{8}$$

2. POHLHAUSEN'S APPROXIMATE SOLUTION OF THE KÁRMÁN INTEGRAL EQUATION

Equation (8) can be solved only when some relation between u and y is assumed. Pohlhausen chose

$$u=Ay+By^2+Cy^3+Dy^4 \tag{9}$$

where A, B, C, and D are determined by the boundary conditions at the surface and at the outer limit of the layer. A parameter δ is introduced such that at $y=\delta$, $u=U$. Having defined δ in this way, we may regard it as the boundary-layer thickness. Since $\frac{\partial U}{\partial y}$ is of a lower order than $\frac{\partial u}{\partial y}$, we may write at $y=\delta$, $\frac{\partial u}{\partial y}=\frac{\partial U}{\partial y}=0$. The supposition has been made that the thickness has a definite finite value; whereas in the physical case u approaches U asymptotically, there being no sharp division between the boundary layer and the region of potential flow. The conditions at δ may be made to simulate the asymptotic case more closely by imposing the condition that the curve of equation (9) shall reach the line $u=U$ with zero curvature. As outer boundary conditions we have therefore

$$u=U,\ \frac{\partial u}{\partial y}=0,\ \frac{\partial^2 u}{\partial y^2}=0 \text{ at } y=\delta$$

As inner boundary conditions we have

$$\frac{\partial^2 u}{\partial y^2}=\frac{R}{2}\frac{\partial p}{\partial x}=-UU'R \text{ at } y=0$$

by equations (4) and (7), since $u=0$ and $v=0$.

When these four conditions are applied, equation (9) becomes

$$u=U\left[\left(2+\frac{\lambda}{6}\right)\frac{y}{\delta}-\frac{\lambda}{2}\left(\frac{y}{\delta}\right)^2+\left(-2+\frac{\lambda}{2}\right)\left(\frac{y}{\delta}\right)^3+\left(1-\frac{\lambda}{6}\right)\left(\frac{y}{\delta}\right)^4\right] \tag{10}$$

where $\lambda=U'\ \delta^2\ R$. Equation (10) represents a family of curves, with δ as parameter, satisfying the inner and outer boundary conditions.

In keeping with the foregoing conditions, the upper limit of the integrals in equation (8) may be written δ instead of ∞ since $U-u$ is zero when y is greater than δ. When this is done and u as given by equation (10) is introduced into equation (8), the integrations with respect to y may be performed. Introducing, for convenience, $\lambda=U'\ z$ and $z=R\ \delta^2$ and making the differentiations with respect to x indicated in (8), the variables being U, U', and z, we obtain finally

$$\frac{dz}{dx}=\frac{0.8\left[-9072+1670.4\lambda-\left(47.4+4.8\frac{UU''}{U'^2}\right)\lambda^2-\left(1+\frac{UU''}{U'^2}\right)\lambda^3\right]}{U(-213.12+5.76\lambda+\lambda^2)} \tag{11}$$

When U, U' and U'' are known functions of x, equation (11) may be solved for z. The method of obtaining the solution is given in section III. For example, at some particular value of x, say x_1, z_1 is found by solving (11). From $z=R\ \delta^2$ and $\lambda=U'\ z$ the particular values $\delta_1=\sqrt{\frac{z_1}{R}}$ and $\lambda_1=U'_1\ z_1$, where U'_1 is the value of U' at x_1, may be found and substituted in (10). The result is

$$u=U_1\left[\frac{\left(2+\frac{\lambda_1}{6}\right)}{\sqrt{z_1}}y\sqrt{R}-\frac{\lambda_1}{2z_1}(y\sqrt{R})^2+\frac{\left(-2+\frac{\lambda_1}{2}\right)}{(\sqrt{z_1})^3}(y\sqrt{R})^3+\frac{\left(1-\frac{\lambda_1}{6}\right)}{z_1^2}(y\sqrt{R})^4\right] \tag{12}$$

where U_1 is the value of U at x_1. Equation (12) is a relationship between u and $y\sqrt{R}$ at the point x_1. Since λ_1, z_1 and δ_1 are constants and $y\sqrt{R}$ is $y\sqrt{\frac{z_1}{\delta_1^2}}$, the $(y\sqrt{R},\ u)$ curve is the same for all values of the Reynolds Number as long as the assumptions underlying the boundary-layer equations are valid. Since the true curve can be represented only approximately by a fourth-degree equation, equation (12) can lead to only an approximate solution.

Separation of the flow from the surface occurs when the fluid in the inner part of the boundary layer has lost sufficient kinetic energy through friction to fail to advance farther into a region of rising pressure. Back of the position where the fluid comes to rest, the higher pressure downstream causes reversed flow and the consequent accumulation of fluid crowds the main flow away from the surface. The point where the fluid comes to rest, just back of which the flow reverses in direction, is the separation point. Analytically, separation will occur when the initial slope of the curve representing equation (10) changes from a positive to a negative value. This occurs when the initial slope is zero; that is, when the first term of equation (10) is zero. The criterion for separation resulting from Pohlhausen's solution is then

$$\lambda = U'\delta^2 R = -12.$$

III. EXPERIMENTAL STUDY OF BOUNDARY LAYER

1. DESCRIPTION OF ELLIPTIC CYLINDER AND HOT-WIRE ANEMOMETER

The elliptic cylinder is of wooden construction, with major and minor axes of 11.78 inches and 3.98 inches, and is 54 inches in length. It was mounted vertically between the upper and lower faces of a 54-inch octagonal wind tunnel, thus extending completely across the tunnel from one face to the opposite face. The surface was made smooth by alternate varnishing and sandpapering and finally by polishing with crocus paper. Around one side 2½ inches below the horizontal mid-section of the tunnel, 16 pressure orifices were inserted for obtaining the pressure distribution over the surface. The connections were copper tubes of 0.04-inch inside diameter extending from the outer surface to the hollow interior of the cylinder and thence to the outside of the tunnel where connection could be made to a manometer. The number and distance of each orifice measured along the surface from the stagnation point are given in the first and second columns of table I.

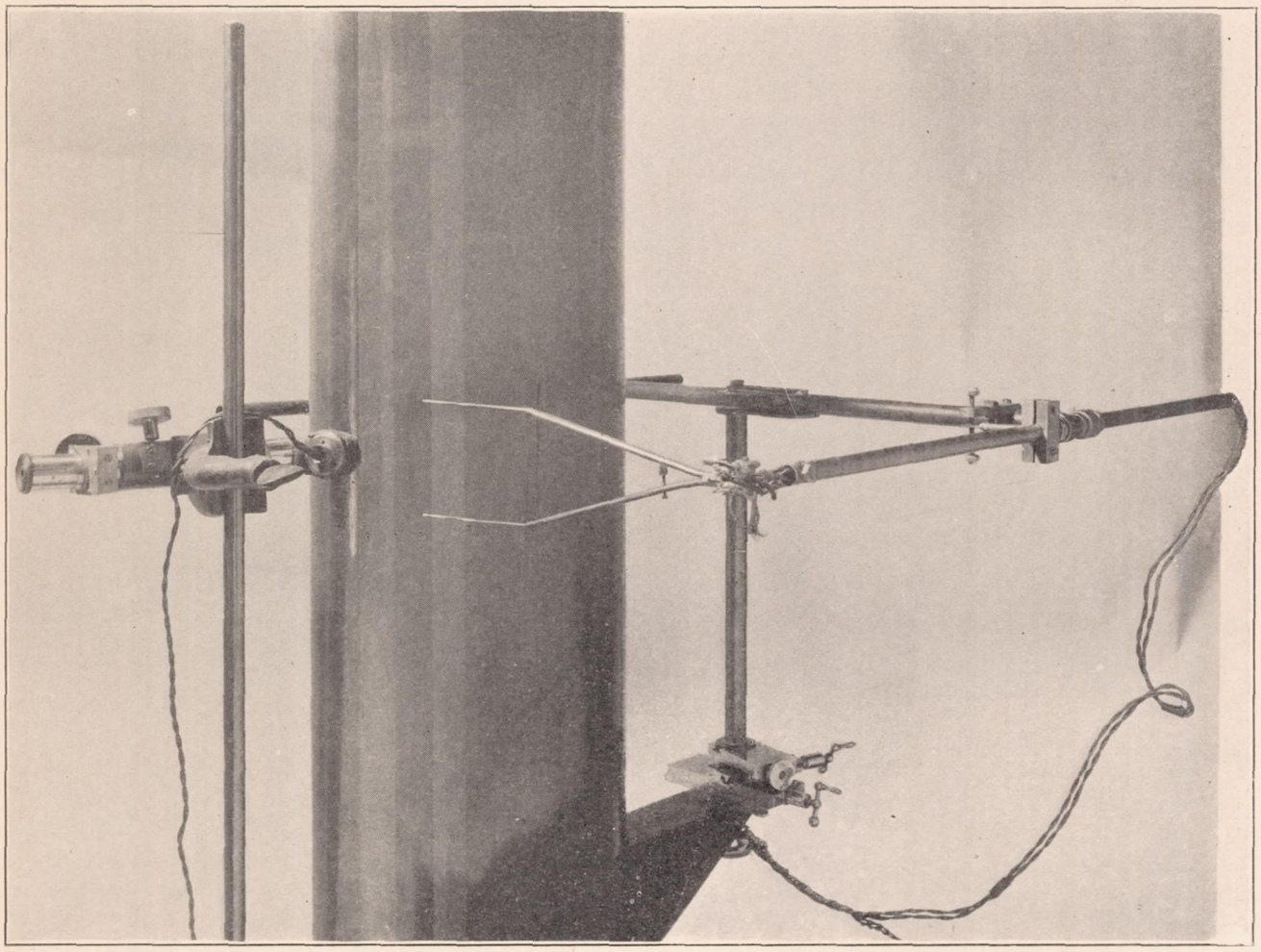

FIGURE 1.—Photograph showing elliptic cylinder and hot-wire anemometer. The microscope as it was set for viewing the wire is also shown.

The hot-wire anemometer may be described best by reference to the photograph (fig. 1). The essential part of the instrument is a platinum wire, 0.002 inch in diameter and 3 inches in length, on the ends of the flexible supporting prongs. The heat loss from this wire when heated by a constant electric current serves

as an indication of the air speed across it. By means of the three micrometer screws in the small lathe head on the bracket at the rear of the cylinder, the wire could be moved in any direction through a distance of about 2 inches. A setting to any position around the surface could be made by readjusting the upper horizontal part of the support.

The microscope and lamp shown in figure 1 were used to determine the distance between the wire and the surface, for a given micrometer reading, by viewing the wire and its reflection in the surface. They were removed when speed measurements were being made.

2. PRESSURE DISTRIBUTION

An inclined benzol manometer, one side of which was open to the still air of the tunnel room and the other

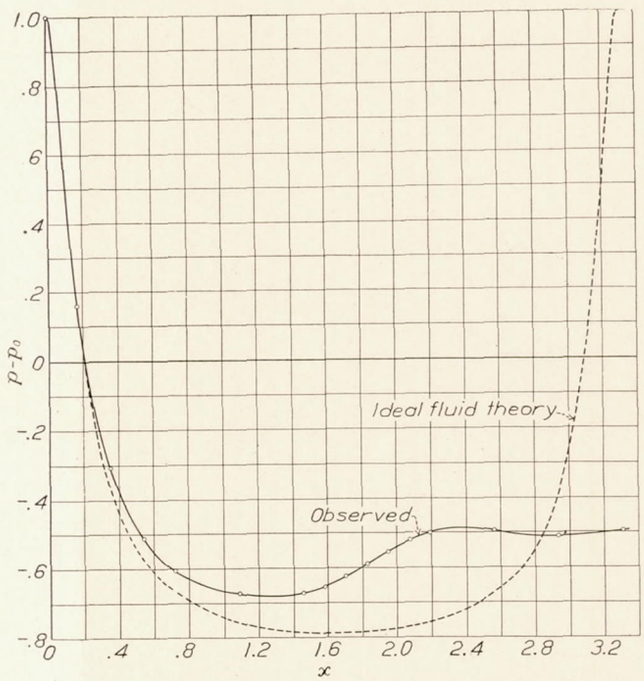

FIGURE 2.—Pressure distribution around one side of elliptic cylinder as determined at 16 pressure orifices.

side connected to a calibrated pressure orifice in the tunnel wall 10 feet ahead of the cylinder, was used in measuring air speed in the tunnel. The movement of the liquid in the manometer was slight, since the speed maintained was low (about 11.5 feet per second), and had to be measured by a traveling microscope provided with a micrometer screw. The difference in pressure between the wall of the tunnel and each of 16 positions about the cylinder was obtained by connecting separately the pressure orifices in the cylinder surface to the side of the manometer previously open. The prevailing drop in static pressure between the tunnel-wall orifice and the leading edge of the cylinder was subtracted from these differences to give $p-p_0$, from which U was computed by means of equation (6).

After a setting of the cylinder with its major axis approximately parallel to the undisturbed air stream, finer adjustment of the orientation was made until the angle of attack was zero as indicated by comparison between the observed pressure distribution over the forward part of the cylinder and that computed from nonviscous fluid theory for zero angle of attack (reference 5). Exact agreement with theory could not be obtained because of the influence of the boundary layer, the blocking of the tunnel stream by the cylinder, and the pressure drop in the tunnel. For making boundary-layer calculations, however, only the actual pressure distribution need be known. It may be remarked that the purpose was to study not the boundary layer on the surface of an elliptic cylinder, but rather the boundary layer on a surface with a known pressure distribution.

The effect of the hot-wire anemometer and support upon the distribution was determined for various settings about the surface with the anemometer lowered until the prongs spanned the orifices. Since the effect

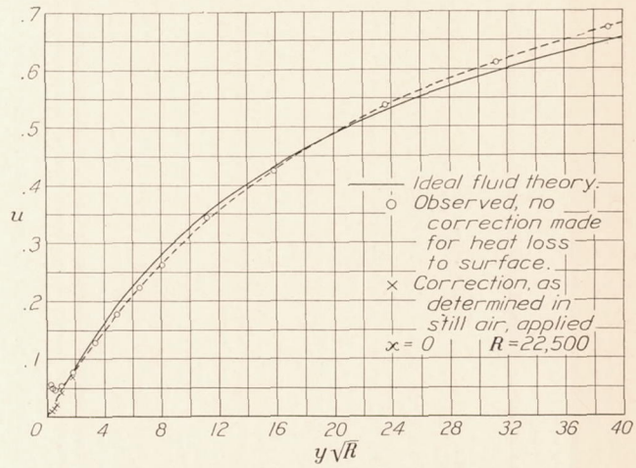

FIGURE 3.—Theoretical and observed speed distributions at stagnation point. The theoretical curve was obtained from ideal fluid theory for the elliptic cylinder at zero angle of attack.

was small in all cases, especially ahead of the prongs, it was neglected. Pressure distributions were measured from time to time during the work as a safeguard against accidental shifting of the cylinder. Good agreement was always obtained. The final results for anemometer and support absent are given in column 3 of table I and in figure 2. In figure 2 the theoretical pressure distribution for flow of a nonviscous fluid is also given.

3. SPEED DISTRIBUTION IN THE BOUNDARY LAYER

The relationship between the rate of cooling of a heated wire and the speed of the air across it is

$$H=A+B\sqrt{S}$$

where H is the heat loss per degree difference in temperature between the wire and the air (in the present experiment, expressed in watts per degree Centigrade), S is the cross-wire air speed, and A and B are functions of the particular wire and the air density. A and B are determined by measuring H at known air speeds. When H is plotted as ordinate and $\sqrt{S}$ as abscissa, the resulting calibration curve is linear. Since A and

B were found to change gradually over a period of time, or suddenly if the wire received rough treatment, it was necessary to calibrate the wire before and after each day's work. Since the hot wire responds equally well to flow in any direction, only the resultant speed

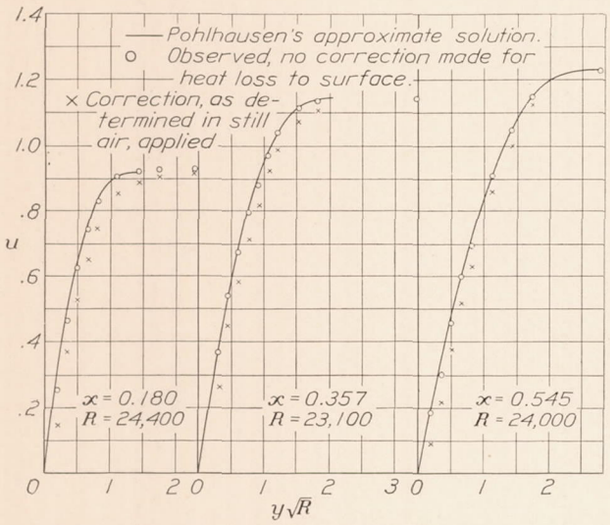

FIGURE 4.—Speed distributions in the boundary layer at three positions as designated by the values of x. Note the better approach to the origin when no correction is made for heat loss to the surface.

can be measured with it. For this reason u and U are termed "speeds" rather than "velocities" when speaking of experimentally determined values. Before the boundary layer separates from the surface the measured speeds are, with good approximation, the x components of velocity. Wherever the flow direction

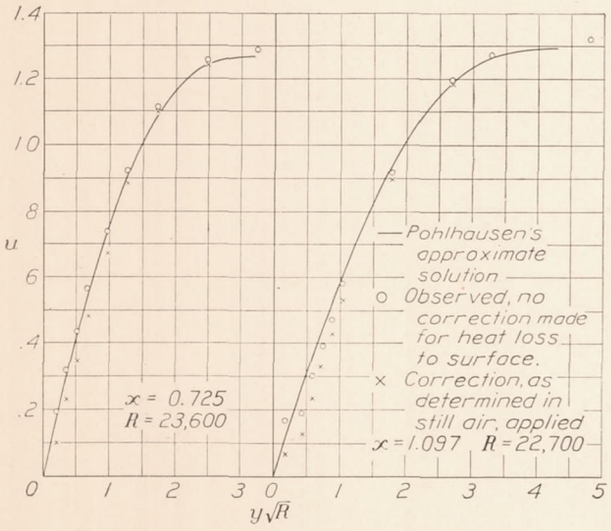

FIGURE 5.—Speed distributions in the boundary layer at two positions as designated by the values of x.

is obviously not that of x, the superscript * will be added, for example, u^*.

Before measurements of speed distribution were made, the effect of the cylinder surface on the heat loss from the hot wire in still air was determined. At 2 millimeters from the surface the cooling effect became perceptible. Within this distance the heat loss to the surface (expressed as $H-H_\infty$, where H_∞ is the heat loss in still air at a great distance from the surface and H is the heat loss near the surface) was determined as a function of the distance y and the temperature difference between the wire and the surroundings. It was recognized at the time that the heat loss to the surface is also a function of the air

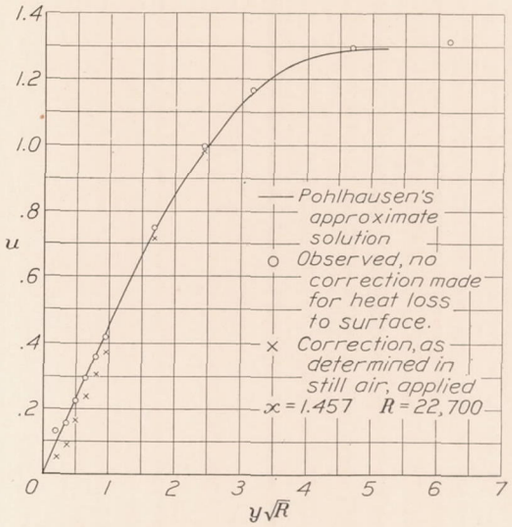

FIGURE 6.—Speed distributions in the boundary layer.

speed at the wire and the gradient in speed between the wire and the surface. Some results of Piercy and Richardson (reference 6) strengthen this view. No means were available, however, for determining this relationship, nor were the results of Piercy and Richardson applicable. Just how and when a cor-

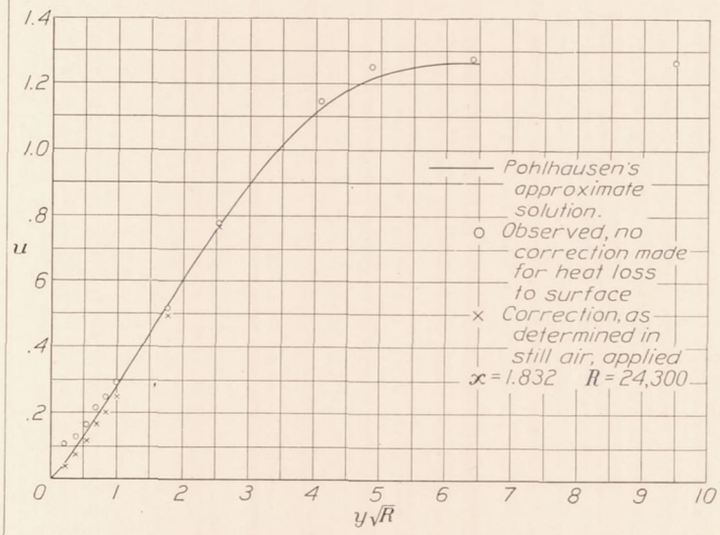

FIGURE 7.—Speed distributions in the boundary layer. Note the better approach to the origin when a correction is made for heat loss to the surface.

rection should be applied to eliminate heat loss to the surface is therefore uncertain. When the smooth approach of the speed to zero at the surface is used as a criterion, the present results indicate that a correction varying as some inverse function of the speed, as well as with distance and temperature difference, should be applied.

Traverses through the boundary layer were made at suitably chosen positions on the surface. At each position measurements of the speed were made from well outside the boundary layer to within 0.2 millimeter of the surface. The intervals moved were read from the scale attached to that one of the three micrometer screws which was employed at the time in moving the wire. The final distance y was determined by counting divisions on the eyepiece scale of the microscope between the center of the wire and its image in the surface. Each time the microscope was set into position for measuring this final distance, the eyepiece scale was calibrated by comparing the change in the number of scale divisions between the wire and its image with the distance through which the wire was moved by the screw. It is estimated that distances so determined have an accuracy of ± 0.04 millimeter.

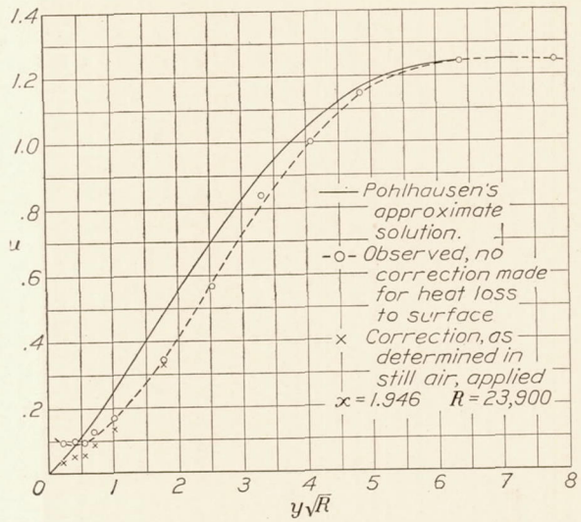

FIGURE 8.—Speed distributions in the boundary layer. Note the better approach to zero when a correction is made for heat loss to surface.

The results are given in figures 3 to 12, inclusive. By means of the $(y\sqrt{R}, u)$ scheme of representation the curves are independent of Reynolds Number. (See sec. II, 2.) Reference to the x and x_b scales of figure 13 will aid the reader to visualize the position of the various distributions. It will be observed that two sets of results are given, those to which a correction for heat loss to the surface as determined in still air has been applied and those for which it has been omitted entirely. Allowing for an uncertainty in $y\sqrt{R}$ of ± 0.06 (± 0.04 mm), the manner of approach to zero will aid in judging where the correction should be applied and where it should not. In figures 4 and 5, because of the high speeds at which the lower points fall, the correction seems to be unnecessary; whereas in figures 6 to 12, with somewhat lower speeds at the lower points, a correction seems to be justified.

In figure 3 a comparison is made between the measured speed distribution at the stagnation point and that computed on the basis of an ideal fluid (reference 5). Although exact agreement is not to be expected because of the tunnel blocking and the effect of the wake, such a comparison serves as an approximate check on the hot-wire measurements.

A clear and precise indication of the position of separation was obtained by allowing smoke to enter the stream slowly through a pressure orifice just back of the separation point. The smoke moved slowly forward (indicating reversed flow) to a definite stopping point. When another orifice farther back of separation was employed, the smoke from it moved forward to the same limiting position. The separation point was thus determined at $x=1.99\pm 0.02$. The experimental curve of figure 8 shows the speed distribution just before separation and that of figure 9 just after. That no marked change appears may be attributed to the fact that the hot-wire anemometer responds equally well to flow in any direction. This uncertainty in direction is indicated by the use of a special symbol u^*, it being understood that the uncertainty exists only on the lower horizontal part of the curves representing flow after separation. Before separation, with u of order 1 and v of order $\delta=0.05$, the assumption that the measured speed is parallel to x is quite good. After separation not only has the velocity reversed in direction near the surface but, in addition, there are probably large normal components where the reversed flow curves outward. If we were to speak of velocities in connection with the experimental curve of figure 9, we would say that the vector representing the velocity turns from a direction parallel to the surface pointing upstream through a little less than 180° pointing downstream in approximately the direction of x_b, as we follow the curve from the origin outward.

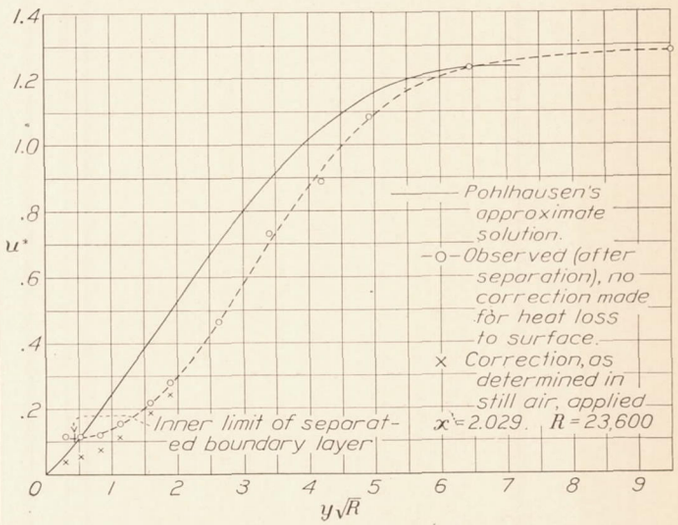

FIGURE 9.—Speed distributions in the boundary layer after separation. The * indicates an uncertainty in the direction of the speed in the wake.

Figures 9, 10, 11, and 12 show traverses of the separated boundary layer and wake. It is apparent that no abrupt change in speed distribution in the layer accom-

panies separation. It must be remembered, however, that u^* is resultant speed and that approximately the same conditions as to direction obtain in figures 10, 11, and 12 as in figure 9. Visual observations with smoke showed that the air motion in the wake fluctuated greatly and that only near the separation point was the reversed flow at all regular. The hot wire shows this persistence of air motion in the wake. The results obtained here are much like those obtained by Linke in his study of the laminar boundary layer separated from a circular cylinder (reference 7). In figure 13 the boundary layer is drawn to the same scale as the elliptic section. The thickness of the layer both on and separated from the surface is taken as the width of the region in which the speed is changing; that is, the length of abscissa between the points of the $(y\sqrt{R}, u)$ curves where the tangents become horizontal. Owing to the asymptotic character of the limits, δ is somewhat arbitrary; but, since the same procedure was used throughout, figure 13 gives a picture of one part of the boundary layer as related to any other and shows the changes that occur.

IV. CALCULATION OF SPEED DISTRIBUTION BY POHLHAUSEN'S APPROXIMATE METHOD

The information required for an evaluation of U, U', and $\frac{UU''}{U'^2}$ as functions of x may all be obtained from the curve of pressure distribution and its first and second derivatives. The derivatives were obtained by the following procedure. From $x=0$ to 1.1, where the theoretical and experimental pressure distributions agree rather closely, a curve of differences was plotted with x as abscissa. The slopes of the difference curve, obtained graphically, were then applied to the theoretical slopes as a correction. In this way errors in determining the true slope entered only into the small correction. For values of x greater than 1.6, where the theoretical and experimental curves bear no resemblance to one another, a graphical determination of the slope of the experimental $(x, p-p_0)$ curve was made directly; and for values of x between 1.1 and 1.6 both the direct and difference methods were used. A curve of $\left(x, \frac{dp}{dx}\right)$ was then plotted and a similar procedure followed in determining $\frac{d^2p}{dx^2}$. The final values are given in columns 4 and 5 of table I. By the formulas (*a*), (*b*), and (*c*) at the foot of table I, U, U' and $\frac{UU''}{U'^2}$ were calculated. Formula (*a*) is the same as equation (6) and (*b*) and (*c*) follow from (*a*) by differentiation and combination. The values of U, U', and $\frac{UU''}{U'^2}$ are given in columns 6, 7, and 8 of table I.

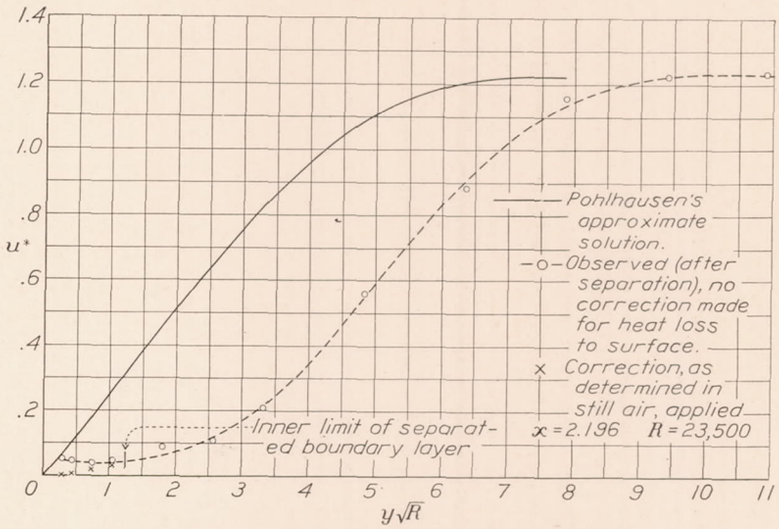

FIGURE 11.—Speed distributions in the boundary layer after separation. The * indicates an uncertainty in the direction of the speed in the wake.

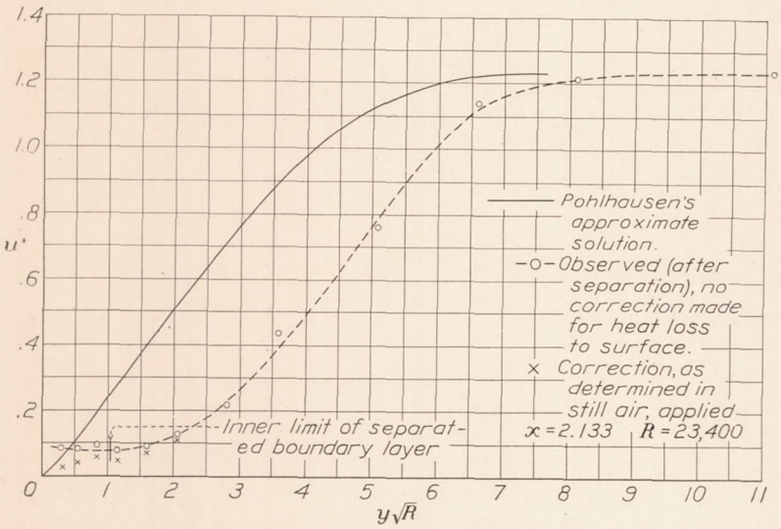

FIGURE 10.—Speed distributions in the boundary layer after separation. The * indicates an uncertainty in the direction of the speed in the wake.

Equation (11) was solved by the isocline method. This method involves computing $\frac{dz}{dx}$ with assumed values of z for various values of x and the accompanying values of U, U', and $\frac{UU''}{U'^2}$. Points of known $\frac{dz}{dx}$ are then located on an (x, z) diagram and a short line drawn through each to indicate the slope at the point. The solution curve is then drawn in, passing through the various points with the slope indicated at each. (See fig. 14.) A procedure more convenient in certain parts of the diagram is to draw lines of constant slope (isoclines) and then draw the solution curve crossing the isoclines with the slope marked on them.

The particular solution curve required is the one that satisfies the boundary conditions at $x=0$, the stagnation point. Since $U=0$ at $x=0$, $\frac{dz}{dx}$ has infinite

values for values of z other than those for which $U'z=\lambda$ is one of the roots of the numerator of equation (11). At $x=0$, $U=0$, the numerator, a cubic in λ, has roots $\lambda_1=7.052$, $\lambda_2=17.80$, $\lambda_3=-72.26$. The corresponding values of z are $z_1=0.89$, $z_2=2.25$, $z_3=-9.13$. At z_1, z_2, and z_3 we find singular points at which $\frac{dz}{dx}$ is indeterminate. A solution curve can then leave the z-axis only at one of the singular points. The singular point at z_3, involving an imaginary δ, is obviously of no interest. It was found that a solution curve leaving the singular point at z_2 led immediately to very large values of δ, entirely out of agreement with experiment. The zero isocline then leaves with zero slope. A little consideration will show that the solution curve must leave the singular point along an isocline whose initial slope equals the value marked on the isocline; in this case the one with zero slope. For the sake of accuracy, the solution curve was determined from a large diagram containing more values of the slope than that shown in figure 14. The values of z and x resulting from the solution are given in table II. From the values of U' and R, λ and δ were calculated. These quantities appear in the same table. The speed distributions were calculated from these values of λ and z.

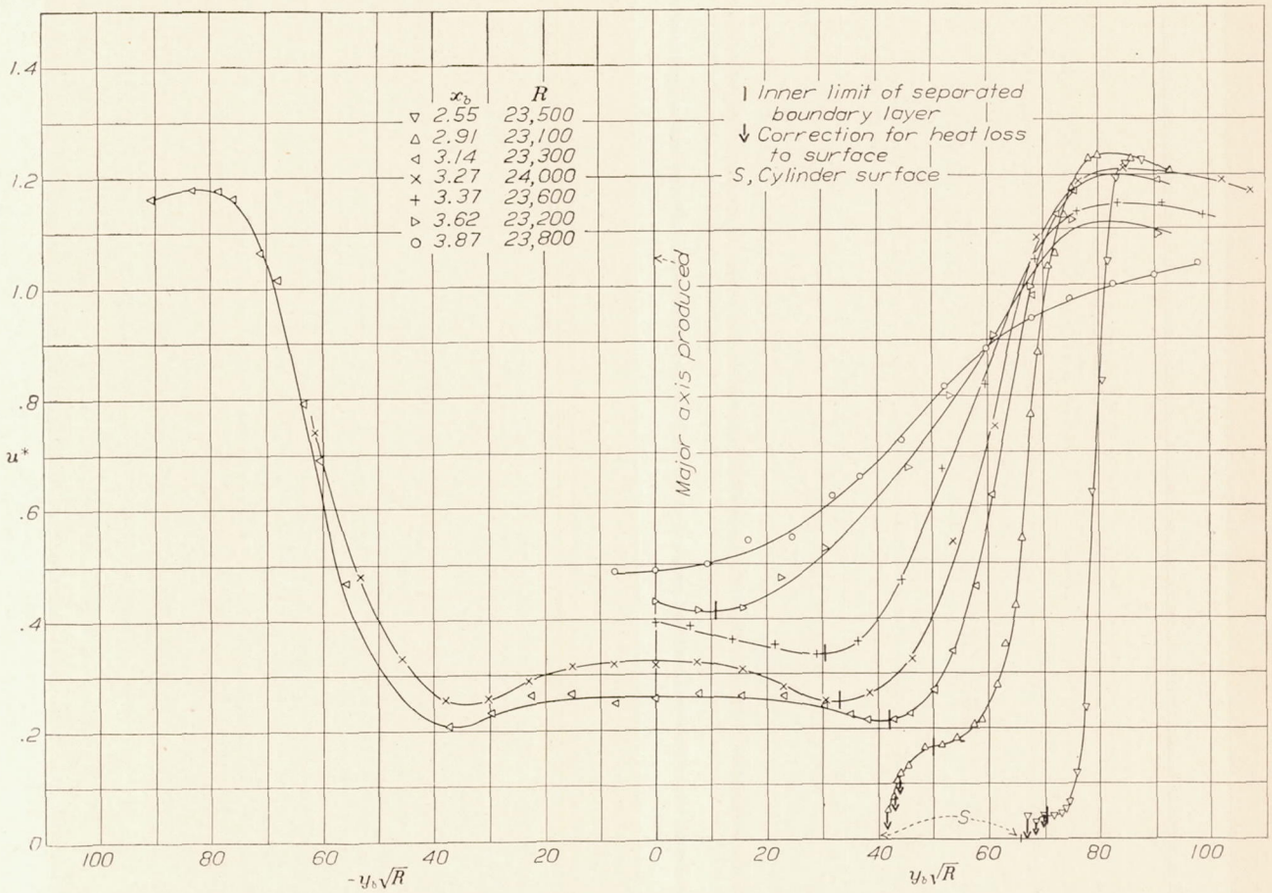

FIGURE 12.—Speed distribution in the separated boundary layer and wake (experimental). The * indicates an uncertainty in the direction of the speed in the wake. y_b means distances normal to the major axis of the ellipse.

The singular point at z_1 was the only one that gave a solution curve in agreement with experiment. The isoclines leaving z_1 have an initial slope given by[2]

$$\left(\frac{dz}{dx}\right)_1=-0.180\left(\frac{dz}{dx}\right)_i.$$

[2] $0.8\left[-9072+1670.4\lambda-\left(47.4+4.8\frac{UU''}{U'^2}\right)\lambda^2-\left(1+\frac{UU''}{U'^2}\right)\lambda^3\right]$ / $U(-213.12+5.76\lambda+\lambda^2)$ = a constant for any one isocline. Differentiating with respect to x and setting $\frac{UU''}{U'^2}=0$, $\frac{d\left(\frac{UU''}{U'^2}\right)}{dx}=0$, $U=0$ for $x=0$; then substituting $\lambda_1=(U')_0 z_1$, we get the result $\left(\frac{dz}{dx}\right)_1=-0.180\left(\frac{dz}{dx}\right)_i$ where $\left(\frac{dz}{dx}\right)_1$ is the initial slope of the isocline whose value is $\left(\frac{dz}{dx}\right)_i$.

V. DISCUSSION OF RESULTS

It will be observed in table II that the boundary layer has an initial thickness of about 0.6 millimeter. It is a matter of conjecture as to whether a true boundary layer really exists at the stagnation point. The measurements indicate that potential flow probably extends to the surface.

Also of note in table II is the absence of any λ less than -5.37. The value $\lambda=-12$ required for separation was not attained. No calculations were made for values of x greater than 2.937, but it is apparent from the value of U' that no z can be reached for which $\lambda=U'z=-12$. Therefore, according to the calcu-

lation, separation does not occur anywhere on the cylinder. As we have seen, separation was found experimentally at $x=1.99$.

The failure of λ to reach sufficiently high negative values is reflected in the growing discrepancy between calculated and observed distributions in figures 8 to 11. As shown by figures 4 to 7, Pohlhausen's method yields good agreement with experiment up to an x of 1.832.

From an estimate of the pressure distribution required to give a calculated value of separation in agreement with experiment, it was at first suspected that the pressure distribution might not have been determined accurately enough in the region where separation occurred. A redetermination with pressure orifices installed in the cylinder at critical points showed that the pressure distribution as originally determined was correct and that as far as $x=2.1$ the

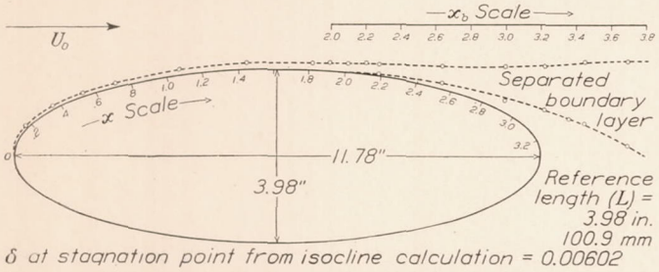

FIGURE 13.—Diagram showing elliptic cylinder and boundary layer in section. This diagram shows the thickness of the boundary layer compared to the size of the ellipse.

experimental curve of figure 2 is definitely fixed both as regards position and shape.

The question arises as to whether Pohlhausen's solution begins to fail after $x=1.832$ or whether the assumptions made in simplifying the general equation of section II cease to be valid. The following table shows that δ changes but little through the interval in x where discrepancies begin to appear. The failure can then hardly be attributed to the growth of δ. J. J. Green (reference 8) has shown for the case of a circular cylinder that the neglected terms become important only at the separation point. Here v probably reaches an order of magnitude near that of u.

x	δ (by experiment)
0.1800	0.009
.357	.014
.545	.019
.725	.023
1.097	.032
1.457	.040
1.832	.044
1.946	.045
2.029	.049

It appears, therefore, that the initial failure is the result of the approximations introduced in Pohlhausen's solution; whereas farther downstream, say at or near the separation point, the failure may be due to the absence of important terms in the basic equations as well.

The only other known test of Pohlhausen's solution is that given by Pohlhausen himself (reference 1) using data obtained by Hiemenz for a circular cylinder in water (reference 9). In this case the calculated separation point was in good agreement with experiment. An examination of the results of Hiemenz shows a steep pressure rise beginning a short distance ahead and extending up to separation. The x, λ curve for the circular cylinder shows a steep fall in the region of separation. Therefore the experimental separation point must be determined very accurately to show that it falls near $\lambda=-12$. Since the foregoing condition does not obtain to so great a degree in the present experiment, the test applied here to the solution in the region of separation is a more sensitive one than that applied by Pohlhausen.

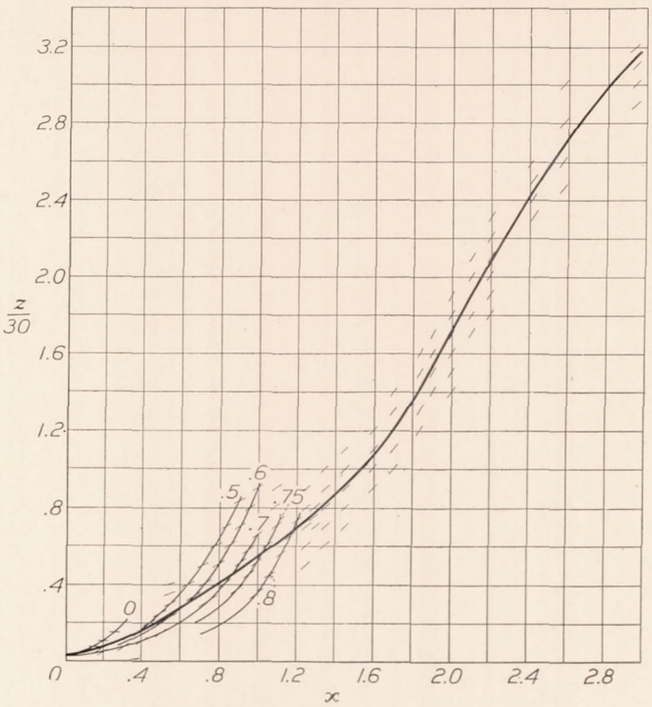

FIGURE 14.—Isocline diagram and solution curve of equation 11.

CONCLUSION

The experimental data presented here show that Pohlhausen's solution may be expected to yield reliable results where the speed in the potential flow is increasing. In the region of decreasing speed, the solution cannot be relied upon to determine the speed distribution, but gives the boundary-layer thickness to a fair degree of approximation. Separation may actually occur where the solution of Pohlhausen fails to give it.

The author wishes to acknowledge his indebtedness to Dr. H. L. Dryden of the National Bureau of Standards for his many valuable suggestions and to Professors K. F. Herzfeld and F. D. Murnaghan of The Johns Hopkins University for their critical reading of the manuscript. The author also wishes to express his appreciation of the assistance given by Mr. W. C.

Mock, Jr., of the National Bureau of Standards in making the measurements.

* * * * *

NATIONAL BUREAU OF STANDARDS,
WASHINGTON, D. C., *December 1, 1934.*

REFERENCES

1. Pohlhausen, K.: Zur näherungsweisen Integration der Differentialgleichung der laminaren Grenzschicht. Z. f. angew. Math. u. Mech., vol. I, 1921, p. 252.
2. Lamb, Horace: Hydrodynamics. Cambridge University Press, 5th ed., 1930, p. 547.
3. Fuchs, R., and Hopf, L.: Handbuch der Flugzeugkunde, vol. II: Aerodynamik, 1922, p. 173.
4. Prandtl, L.: Proc. 3d Internat. Math. Congress, Heidelberg, 1904. Reprinted in Vier Abhandlungen zur Hydrodynamik und Aerodynamik. (Kaiser Wilhelm-Institut für Strömungsforschung, Göttingen, 1927.)
5. Zahm, A. F.: Flow and Drag Formulas for Simple Quadrics. T. R. No. 253, N. A. C. A., 1927.
6. Piercy, N. A. V., and Richardson, E. G.: On the Flow of Air Adjacent to the Surface of an Aerofoil. R. & M. No. 1224, British A. R. C., 1928.
7. Linke, Werner: Neue Messungen zur Aerodynamik des Zylinders, insbesondere seines reinen Reibungswiderstandes. Physik. Zeitschr., vol. 32, 1931, p. 900.
8. Green, J. J.: The Viscous Layer Associated with a Circular Cylinder. R. & M. No. 1313, British A. R. C., 1930.
9. Hiemenz, K.: Die Grenzschicht an einem in der gleichförmigen Flüssigkeitsstrom eingetauchten geraden Kreiszylinder. Dinglers Polytechnisches Journal, vol. 326, 1911, p. 322.

TABLE I.—DATA DERIVED FROM PRESSURE DISTRIBUTION FOR CARRYING OUT SOLUTION OF POHLHAUSEN

Orifice number	x	$p-p_0$	$\frac{dp}{dx}$	$\frac{d^2p}{dx^2}$	U	U'	$\frac{UU''}{U'^2}$
1	0	1.000	0	−125.4	0	7.92	0
2	.175	.163	−4.43	26.7	.914	2.42	−3.28
	.260	−.115	−2.56	15.9	1.055	1.213	−6.42
3	.357	−.307	−1.571	7.80	1.142	.688	−9.27
	.460	−.440	−1.010	4.30	1.200	.421	−13.14
4	.545	−.513	−.719	2.72	1.230	.292	−16.9
5	.725	−.605	−.354	1.38	1.266	.140	−36.4
	.950	−.657	−.150	.60	1.286	.0583	−89.4
6	1.097	−.672	−.0633	.485	1.293	.0245	−406.0
	1.250	−.677	−.0050	.44	1.295	.00193	−59000.0
	1.350	−.677	.030	.47	1.295	−.0116	−1750.0
7	1.457	−.671	.086	.49	1.292	−.0332	−226.0
8	1.581	−.655					
	1.600	−.650	.180	.52	1.284	−.0701	−54.0
	1.700	−.627	.24	.50	1.275	−.0941	−29.26
9	1.704	−.626					
10	1.832	−.592	.306	0	1.261	−.121	−1.0
	1.900	−.569	.30	−.30	1.252	−.120	9.45
11	1.957	−.553					
	2.000	−.540	.25	−.60	1.240	−.101	28.6
12	2.079	−.523					
	2.100	−.516	.20	−.70	1.230	−.0813	52.1
13	2.196	−.501	.15	−.70	1.225	−.0592	97.0
14	2.568	−.497	−.064	−.20	1.223	.026	145.0
15	2.937	−.509	−.001	.2	1.228	.00041	-7.1×10^5
16	3.307	−.495	.08	.2	1.222	−.03	−134.0

(a) $U=\sqrt{1-(p-p_0)}$.

(b) $U'=-\frac{1}{2U}\frac{dp}{dx}$.

(c) $\frac{UU''}{U'^2}=-\frac{2U^2\frac{d^2p}{dx^2}}{\left(\frac{dp}{dx}\right)^2}-1$.

TABLE II.—VALUES OF λ AND δ CALCULATED BY POHLHAUSEN'S SOLUTION AT POSITION x AND FOR REYNOLDS NUMBER R

[Boundary-layer thickness in millimeters=101.1 δ]

x	U'	z	λ	R	δ
0	7.92	0.890	7.052	24,500	0.00602
.180	2.42	1.91	4.63	24,400	.00884
.357	.688	4.22	2.90	23,500	.0134
.545	.292	7.26	2.12	24,000	.0174
.725	.140	10.47	1.46	23,600	.0211
1.097	.0245	18.36	.449	22,700	.0284
1.457	−.0332	27.48	−.912	22,700	.0348
1.832	−.121	42.0	−5.10	24,300	.0415
1.946	−.111	48.5	−5.37	23,900	.0447
2.029	−.095	52.9	−5.03	23,600	.0474
2.133	−.075	58.5	−4.39	23,400	.0500
2.196	−.059	61.7	−3.65	23,500	.0512
2.568	.26	80.3	2.10	23,500	.0584
2.937	.00041	93.9	.038	23,100	.0638

$\lambda=U'z \quad \delta=\sqrt{\frac{z}{R}}$

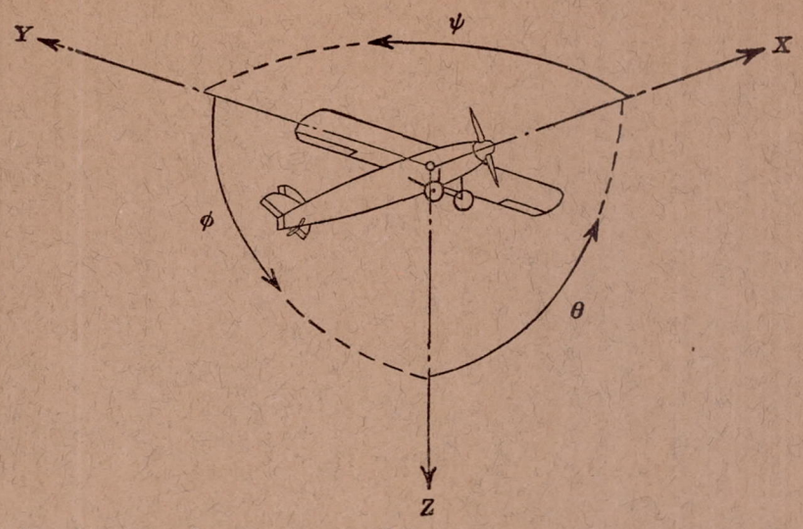

Positive directions of axes and angles (forces and moments) are shown by arrows

Axis		Force (parallel to axis) symbol	Moment about axis			Angle		Velocities	
Designation	Symbol		Designation	Symbol	Positive direction	Designation	Symbol	Linear (component along axis)	Angular
Longitudinal	X	X	Rolling	L	$Y \longrightarrow Z$	Roll	ϕ	u	p
Lateral	Y	Y	Pitching	M	$Z \longrightarrow X$	Pitch	θ	v	q
Normal	Z	Z	Yawing	N	$X \longrightarrow Y$	Yaw	ψ	w	r

Absolute coefficients of moment

$C_l = \frac{L}{qbS}$ (rolling) $\quad C_m = \frac{M}{qcS}$ (pitching) $\quad C_n = \frac{N}{qbS}$ (yawing)

Angle of set of control surface (relative to neutral position), δ. (Indicate surface by proper subscript.)

4. PROPELLER SYMBOLS

D, Diameter

p, Geometric pitch

p/D, Pitch ratio

V', Inflow velocity

V_s, Slipstream velocity

T, Thrust, absolute coefficient $C_T = \frac{T}{\rho n^2 D^4}$

Q, Torque, absolute coefficient $C_Q = \frac{Q}{\rho n^2 D^5}$

P, Power, absolute coefficient $C_P = \frac{P}{\rho n^3 D^5}$

C_s, Speed-power coefficient $= \sqrt[5]{\frac{\rho V^5}{P n^2}}$

η, Efficiency

n, Revolutions per second, r.p.s.

Φ, Effective helix angle $= \tan^{-1}\left(\frac{V}{2\pi r n}\right)$

5. NUMERICAL RELATIONS

1 hp. = 76.04 kg-m/s = 550 ft-lb./sec.

1 metric horsepower = 1.0132 hp.

1 m.p.h. = 0.4470 m.p.s.

1 m.p.s. = 2.2369 m.p.h.

1 lb. = 0.4536 kg.

1 kg = 2.2046 lb.

1 mi. = 1,609.35 m = 5,280 ft.

1 m = 3.2808 ft.